PHYSICAL REVIEW C **66**, 021301(R) (2002)

Evidence for $^{16}O+^{16}O$ cluster bands in ^{32}S

Shigeo Ohkubo and Kotoe Yamashita
Department of Applied Science and Environment, Kochi Women's University, Kochi 780-8515, Japan
(Received 18 March 2002; published 2 August 2002)

Evidence for the existence of the lowest $N=24$ and $N=28$ cluster bands with the $^{16}O+^{16}O$ cluster structure in ^{32}S is shown from the viewpoint of unified description of bound and scattering states of the $^{16}O+^{16}O$ system. The $^{16}O+^{16}O$ cluster band structure, the gross structure of the 90° excitation function for $^{16}O+^{16}O$ elastic scattering, and the Airy minima are understood in a unified way. The existence of the unobserved $N=26$ higher nodal band is predicted.

DOI: 10.1103/PhysRevC.66.021301 PACS number(s): 21.60.Gx, 24.10.Ht, 25.70.Bc, 27.30.+t

The concept of clustering in nuclei is very useful and important. In light- and medium-weight nuclei the α-cluster model has been very successful [1]. This model describes not only the spectroscopic properties of bound states but also scattering states in a unified way. In fact, the α-cluster structure of ^{44}Ti and α-particle scattering from ^{40}Ca in a wide range of incident energy can be described by a deep optical potential [2]. The same picture has been successfully extended to much heavier nuclei of ^{94}Mo and ^{212}Po [3].

The $^{16}O+^{16}O$ system is the most typical heavier cluster analog to the $\alpha+\alpha$ cluster in ^{8}Be. A large number of investigations [4] have been devoted to the system and $^{16}O+^{16}O$ molecular resonances have been observed in elastic scattering, fusion reactions, and transfer reactions. To reveal the $^{16}O+^{16}O$ cluster structure in ^{32}S, many theoretical approaches, such as the microscopic cluster model calculations with resonating group method (RGM) and generator coordinate method (GCM) [5–7], have been made. Up to now, to our knowledge, in spite of many efforts, the band structure with the $^{16}O+^{16}O$ configuration in ^{32}S has not been established. For example, at what energy the lowest $^{16}O+^{16}O$ cluster band starts and how many rotational bands exist, have not been solved yet. The purpose of this paper is to show that the $^{16}O+^{16}O$ cluster bands exist in ^{32}S and reveal their properties from the unified description of bound and scattering states of the $^{16}O+^{16}O$ system.

Ikeda's threshold rule has been a useful guide in knowing at what energy the lowest cluster structure appears in nuclei. However, as for the $^{16}O+^{16}O$ cluster structure in ^{32}S, experimentally the cluster band has not been clearly confirmed. On the other hand, theoretical studies using GCM and RGM located the lowest cluster band at different energies depending on the effective force used. According to Ref. [5], which uses Volkov force No. 1, and Refs. [6], which uses Brink-Boeker force, each theory gives only one rotational band, which starts at $E_{\mathrm{c.m.}}=10.36$ MeV and 6.6 MeV, respectively, and the gross structure of the 90° excitation function for $^{16}O+^{16}O$ scattering is due to the band. On the other hand, according to Ref. [7], which uses density-dependent forces as well as Volkov force, its theory gives more than two rotational bands: the first band starts near the threshold energy and the second one is responsible for the gross structure. The energy surface of the GCM calculation [6] or the equivalent potential of the RGM [7] was consistent with the phenomenological shallow potential [8–10] obtained from the systematic analysis of elastic $^{16}O+^{16}O$ scattering. Many other theoretical models also supported the shallow potential.

It was shown in Ref. [11] that the $^{16}O+^{16}O$ elastic scattering and fusion cross sections can be described by a *J-dependent* deep real potential with $J_V=307$ MeV fm^3, which is consistent with the RGM result, $J_V=306$ MeV fm^3 [12] (this belongs to a shallower family as discussed below). However, the calculated rms radius of the potential, 4.45 fm, was inconsistent with the RGM result, 3.8 fm. (Kondō *et al.* [13] also considered the depth of potential by taking into account the dispersion relation.) Using the inversion technique, Ait-Thaler *et al.* [14] pointed out that this inconsistency is due to its *J-dependent* character of the potential. They also suggested that the potential for the $^{16}O+^{16}O$ system must not necessarily have *J dependence*. In fact, in the $\alpha+^{40}$Ca and $\alpha+^{16}$O systems the global potentials did not need any *J* dependence [2]. Therefore it was important to make clear whether *J* dependence is essential for the $^{16}O+^{16}O$ system, unlike the $\alpha+$nucleus systems, or a *J*-independent deep potential can describe the heavy-ion system in a wide range of energies.

In the 1990s, rainbow scattering of $^{16}O+^{16}O$ scattering was measured systematically and higher-energy data could solve the discrete ambiguities of the deep potential. Systematic analysis of the higher-energy data between $E_L=124$ and 1120 MeV by Khoa *et al.* [16] showed clearly that the angular distributions can be described well by a folding-type diffuse deep potential (no *J* dependence) with the family of $J_V=340$ MeV fm^3. Recent Strasbourg data of $^{16}O+^{16}O$ elastic scattering between $E_L=75$–124 MeV [15] also showed that this potential was successful. Thus, the global potential for the $^{16}O+^{16}O$ system has been uniquely established. This situation is very similar to the one for the $\alpha+^{40}$Ca in the 1980s where the unique global potential has been determined from the systematic analysis of elastic α scattering from ^{40}Ca: the potential was also shown to describe the fusion data as well. The unified description of bound and scattering states of the $\alpha+^{40}$Ca system predicted the existence of the $N=13$, $K=0^-$ α-cluster band [2], which is a parity doublet partner of the ground band of ^{44}Ti and was observed later in the α-transfer experiment [17].

However, for the $^{16}O+^{16}O$ system, different from the ^{44}Ti case, the ground state of the composite system ^{32}S, which is 16.54 MeV below the $^{16}O+^{16}O$ threshold, does not

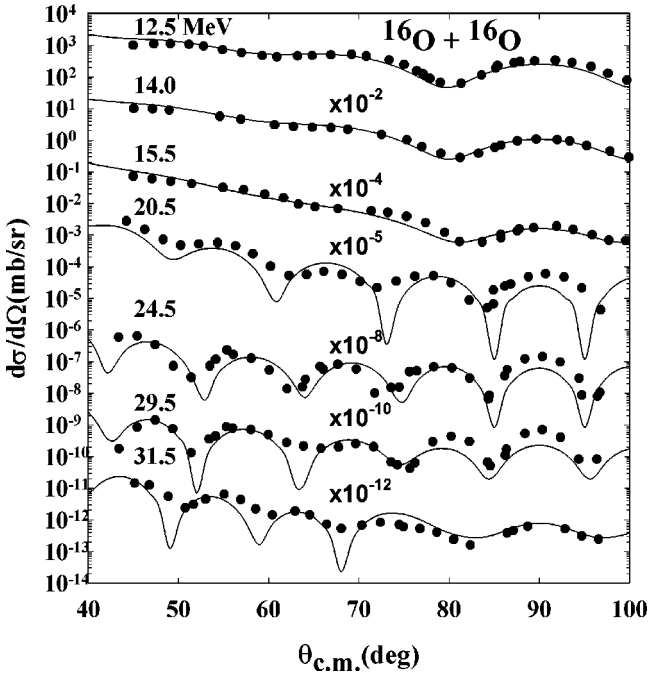

FIG. 1. Comparison of the calculated angular distributions of $^{16}O+^{16}O$ elastic scattering with the data [9].

have the $^{16}O+^{16}O$ configuration. Furthermore, the lowest band with the $^{16}O+^{16}O$ configuration has not been confirmed in experiment. This situation seems to have hampered attempts to try to unify bound and scattering states of the $^{16}O+^{16}O$ system to reveal the cluster structure in ^{32}S. However, recent understanding of the Airy oscillations [15,16,18] observed in $^{16}O+^{16}O$ elastic scattering urges us to study whether the viewpoint of unified understanding is applicable to ^{32}S like ^{44}Ti and ^{20}Ne or not. This is a very important long-standing problem to be solved because if it is shown to be successful in this typical system, it means that this unification cannot be limited to the $^{16}O+^{16}O$ system only and could be applicable to other heavy-ion systems such as the $^{16}O + ^{12}C$ cluster structure in ^{28}Si.

To see how the potential obtained in the energy range of $E_{\text{c.m.}}=37.5$ MeV ($E_L=75$ MeV) to 560 MeV ($E_L=1120$ MeV) can describe the low-energy data between $E_{\text{c.m.}}=12.5$ MeV and 31.5 MeV, which have been usually described by shallow potentials or a J-dependent deep potential [11], we have analyzed the $^{16}O+^{16}O$ scattering starting from a potential determined by Nicoli [19] at $E_{\text{c.m.}}=37.5$ MeV ($V_0=412$ MeV, $R_V=3.97$ fm, $a_R=1.492$ fm), which has a Woods-Saxon squared form factor for real and imaginary parts. The calculated angular distributions are shown in Fig. 1 in comparison with the experimental data. The potential parameters in Table I do not change very much from the original one at $E_{\text{c.m.}}=37.5$ MeV [19] and belongs to the same family. This shows that the deep potential is valid up to the very low energy near the Coulomb barrier.

In order to know the properties of the resonances and bound states supported by this deep potential, the complex scaling method [20] has been used. In Fig. 2 the energy levels calculated with the potential at $E_{\text{c.m.}}=37.5$ MeV are shown in comparison with the experimental data. The $N=24$ band, which is located about 8 MeV below the threshold, is the lowest Pauli-allowed band. The rotational constant k estimated from the lowest spin to the highest one is $k=52$ keV. The second $N=26$ rotational band with $k=55$ keV, which starts from about 3 MeV, has a width of less than 5 keV. The $N=28$ band with $k=59$ keV, which starts from about 10 MeV, has a width of 0.19–1.7 MeV. The three $N=24$, 26, and 28 bands have almost the same rotational constant. The $N=30$ band with $k=68$ keV starts near the Coulomb barrier and is in broad resonance with the width of several MeV. The $N=32$ band has a width of about 10–20 MeV.

The three gross structures of the 90° excitation function at $E_{\text{c.m.}}=20$–30 MeV in Fig. 3, which was assigned as the $N=24$ band resonances in Refs. [5,6] and the $N=26$ band resonances in Ref. [7], are found to be due to the 14^+, 16^+, 18^+ resonances of the $N=28$ band. As indicated in Fig. 3 , the peaks of the 90° excitation function [9,21] are assigned as follows: 12^+ (17.5 MeV), 14^+ (21 MeV), 16^+ (24.5 MeV), 18^+ (29 MeV), 20^+ (33.5 MeV), 22^+ (38 MeV), 24^+ (43 MeV), 26^+ (51 MeV), and 28^+ (57 MeV), which show the $J(J+1)$ behavior with $k=50$ keV and correspond well to our $N=28$ band as seen in Fig. 2. The lower spin states observed in transfer reactions (also in precise elastic scattering) [22,23], 2^+ (9.7 MeV), 4^+ (10.7 MeV), 6^+ (11.3 MeV), 8^+ (12.0 MeV), and 10^+ (15.8 MeV), correspond well to our band (Fig. 2). It is surprising that the calculated energies of the $N=28$ band corre-

TABLE I. Optical potential parameters in the standard notation and volume integrals per nucleon pair.

$E_{\text{c.m.}}$ (MeV)	V_0 (MeV)	R_V (fm)	a_R (fm)	J_V (MeV fm^3)	W_0 (MeV)	R_I (fm)	a_I (fm)	J_W (MeV fm^3)
12.5	410	4.03	1.35	332	95	3.10	0.275	4.2
14.0	410	4.03	1.25	325	95	3.10	0.275	4.2
15.5	410	4.03	1.35	332	95	3.10	0.275	4.2
20.5	408.5	3.99	1.552	340	90	3.15	0.275	4.2
24.5	410	3.99	1.55	341	90.5	3.65	0.275	6.7
29.5	410	4.08	1.2	333	90.5	3.28	0.365	4.6
31.5	410	4.08	1.2	333	85	3.63	1.62	14.9

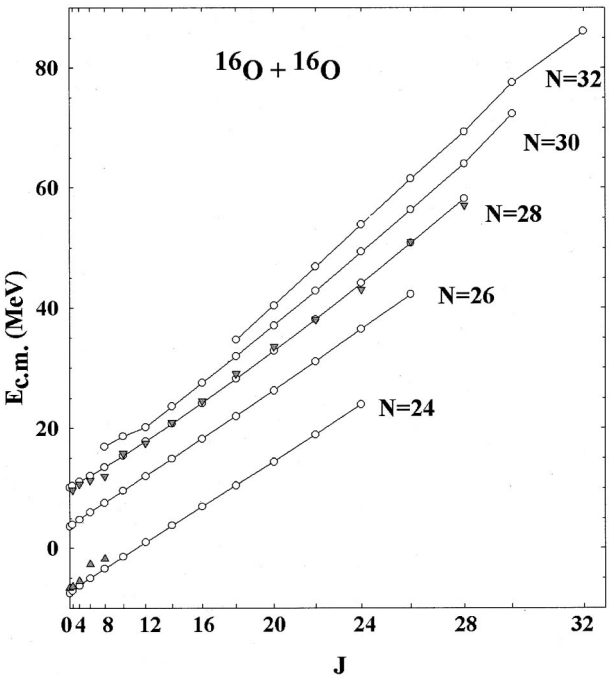

FIG. 2. $^{16}O+^{16}O$ cluster bands calculated in the complex scaling method (circles) are compared with the experimental data (triangles) of Refs. [22, 23, 27, 28] and the marked resonances in Fig. 3. See also the text.

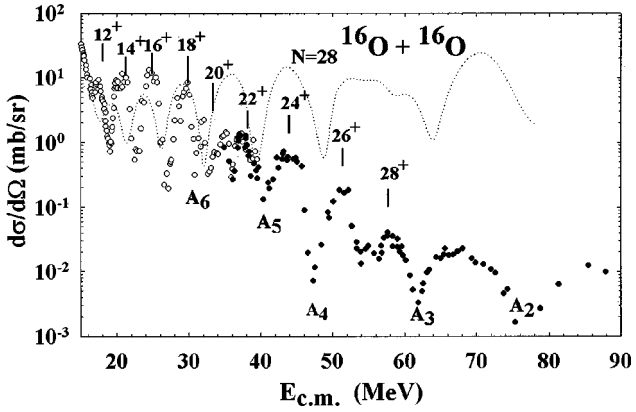

FIG. 3. Candidates of the $N=28$ band are indicated to the experimental data (open circles, Ref. [9] and filled circles, Ref. [21]) of 90° excitation function for $^{16}O+^{16}O$ elastic scattering. Excitation function calculated with the fixed potential at $E_{c.m.}=37.5$ MeV [19] is shown by dotted lines.

spond very well to the experimental data without any adjustment. Although the band head 0^+ state has not been reported in experiment, it seems that there is an indication of a peak in the experimental 90° excitation function near $E_{c.m.}=9.6$ MeV [22]. Because our calculation predicts the band head 0^+ state around this energy region, 10.1 MeV, we hope that it will be searched for in experiment.

It is reminded that in ^{40}Ca and ^{44}Ti the observed α-cluster $N=13$ $K=0^-$ band states and the higher nodal $N=14$ band states are fragmented [17,24]. The fragmentation will become more significant in heavier systems like the $^{16}O+^{16}O$ bands. In fact many states, which are considered to have the $^{16}O+^{16}O$ molecular resonances, have been reported [25]: 10^+ (14.35, 14.57, 14.79, 15.1, 15.2, 15.8, 15.83, 15.9, 16.32, 17.31, 17.67 MeV) 12^+ (16.9, 17.3, 17.9 MeV), and 14^+ (19.8 MeV). Recently, Curtis *et al.* [26] observed new states: 16.42 MeV (10^+ or 12^+), 18.15 MeV (12^+ or 14^+), 19.10 MeV (12^+ or 14^+), 21.01 MeV (14^+ or 16^+), and 21.78 MeV (14^+ or 16^+). The centroids of the above 10^+, 12^+, and 14^+ states are located on the $N=28$ band and agree very well with the corresponding resonance energies marked in Fig. 3. The observed $k=42$–49 keV is in agreement with that of the $N=28$ rather than that of the $N=30$ band. The molecular states, 10^+, 12^+, 14^+, and 16^+ observed by Curtis may be fragmented from the $N=28$ band.

In Fig. 3 the deep Airy minima (A_2–A_6) caused by the interference between far-side internal wave, to which the high-spin members of the $N=30$ and $N=32$ bands contribute, and far-side barrier wave are clearly seen. A_6 is the highest order for the $^{16}O+^{16}O$ system and A_1 is located at 100 MeV. The mechanism of this Airy structure is discussed in detail in Ref. [18]. We notice in Fig. 3 that below the A_3 Airy minimum at 62 MeV, where both the $N=28$ and $N=30$ bands are involved, the broad peaks are fragmented and the spacing between the peaks becomes narrower. Because of widths too large, the calculated states of the $N=30$ and $N=32$ bands in Fig. 2 are difficult to be seen as a clear peak in the excitation function. The excitation function calculated with the potential at $E_{c.m.}=37.5$ MeV [19] (with reduced $W_0=25$ MeV) is shown. This fixed ''average'' potential without any energy dependence both for real and imaginary parts describes the essential structure of the experimental data.

The lowest Pauli-allowed cluster band with $N=24$ appears at 7.5 MeV below the threshold, i.e., $E_x=9.0$ MeV in excitation energy. Experimentally, the band has not been established. In Ref. [27] three $^{16}O+^{16}O$ quasimolecular bands with $k=91$–109 keV, which show the $J(J+1)$ behavior, were suggested in $E_x=11$–17 MeV. The $k=52$ keV of our $N=24$ band disagrees with the ones extracted from the data. Also, theory cannot give three $K=0^+$ bands with the $^{16}O+^{16}O$ configuration in this energy region. In Ref. [27] it was argued that the band obtained in the RGM could correspond to the observed band because the calculated $k=60$–70 keV by Ando *et al.* [7] is not far from the experimental data: However, as mentioned already, we know that the RGM calculation [7] adopted an interaction that belongs to a wrong, shallower family, giving $J_V=302$ MeV fm^3 at $E_L/A=10$ MeV for its equivalent local potential [12]. Kondō *et al.* [11] have discussed the possible $N=24$ band of Ref. [27] using a J-dependent real potential, whose J_V of the equivalent J-independent local potential ranges from 291 MeV fm^3 to 326 MeV fm^3 [14]. However, it is difficult to reconcile the k with the J-dependent potential.

How one can reconcile the $k=91$–109 keV of the experimental data with the present cluster model prediction? We notice that many 0^+, 2^+, 4^+, and 6^+ states have been observed in this energy region [28,27]: 0^+; $E_x=$ 8.507, 9.983, 10.457, 10.787 MeV (centroid 9.93 MeV): 2^+; $E_x=$ 8.690, 8.861, 9.464, 9.711, 9.992, 10.104, 10.510, 10.520, 10.696,

TABLE II. Calculated energy $E_{\mathrm{c.m.}}$ (MeV), rms radii (fm), and $B(E2:J\rightarrow J-2)$ (e^2 fm^4) values of the $N=24$ band.

J^π	$E_{\mathrm{c.m.}}$	$\sqrt{\langle R^2\rangle}$	$B(E2:J\rightarrow J-2)$
0^+	-7.50	4.41	
2^+	-7.10	4.41	482
4^+	-6.26	4.40	682
6^+	-5.02	4.39	735
8^+	-3.40	4.36	741
10^+	-1.39	4.33	721
12^+	0.99	4.29	680
14^+	3.77	4.23	622
16^+	6.94	4.16	547
18^+	10.53	4.08	459
20^+	14.56	3.98	358
22^+	19.01	3.87	245
24^+	23.90	3.75	126

10.757, 10.792, and 10.827 MeV (centroid 10.131 MeV): 4^+; $E_x=9.065$, 10.276, 11.70, and 13.04 MeV (centroid 11.020 MeV): 6^+; $E_x=12.76$, 13.76, and 15.20 MeV (centroid 13.91 MeV). (In Fig. 2 the centroids are plotted by triangles.) As for the 8^+ state, only one is observed at 14.81 MeV [27]. The derived $k=33$–64 keV (average $k=49$ keV) for the centroid of the observed states agrees well with the present prediction $k=52$ keV. The observed states may be considered to be fragmented from the $N=24$ ^{16}O+^{16}O cluster band in Fig. 2. In Table II, $B(E2)$ values and rms radii for the $N=24$ band calculated in the bound-state approximation are given. The band has a cluster structure and shows antistretching as seen in ^{20}Ne and ^{44}Ti. The $B(E2)$ values are enhanced very much and it is desirable to observe the strong cascade transitions. The $N=26$ higher nodal band is inevitably predicted between the $N=24$ and $N=28$ bands, just above the threshold energy. As no experimental counterpart has been observed, observing the band is highly desired.

To summarize, we have shown that the bound and scattering states of the ^{16}O+^{16}O system can be described in a unified way by using a deep potential, which describes high-energy rainbow scattering as well as low-energy scattering near the Coulomb barrier. It was shown that the lowest $N=24$ and the $N=28$ ^{16}O+^{16}O cluster bands in ^{32}S exist in experiment being fragmented. The existence of the unobserved $N=26$ higher nodal band was predicted. This unification may be applicable to other heavy-ion systems.

[1] S. Ohkubo, Prog. Theor. Phys. Suppl. **132**, (1998).
[2] F. Michel, G. Reidemeister, and S. Ohkubo, Phys. Rev. Lett. **57**, 1215 (1986); Prog. Theor. Phys. Suppl. **132**, 7 (1998).
[3] S. Ohkubo, Phys. Rev. Lett. **74**, 2176 (1995).
[4] P.E. Hodgson, *Nuclear Heavy Ion Reactions* (Clarendon, Oxford 1978); R. Bock, *Heavy Ion Collisions*, Vol. 1 (North-Holland, Amsterdam, 1979); *ibid.*, Vol. 2 (North-Holland, Amsterdam, 1980).
[5] H. Friedrich, Nucl. Phys. **A224**, 537 (1974).
[6] D. Baye *et al.*, Nucl. Phys. **A258**, 157 (1976); **A276**, 354 (1977).
[7] T. Ando *et al.*, Prog. Theor. Phys. **61**, 101 (1979); **64**, 1608 (1980).
[8] R.H. Siemssen *et al.*, Phys. Rev. Lett. **19**, 369 (1967); **20**, 175 (1968).
[9] J.V. Maher *et al.*, Phys. Rev. **188**, 1665 (1969).
[10] A. Gobbi *et al.*, Phys. Rev. C **7**, 30 (1973).
[11] Y. Kondō *et al.*, Phys. Lett. B **227**, 310 (1989).
[12] T. Wada *et al.*, Prog. Theor. Phys. **80**, 488 (1988).
[13] Y. Kondō *et al.*, Phys. Lett. B **242**, 340 (1990).
[14] A. Ait-Tahar *et al.*, Nucl. Phys. **A542**, 499 (1992).
[15] M.P. Nicoli *et al.*, Phys. Rev. C **60**, 064608 (1999).
[16] Dao T. Khoa *et al.*, Nucl. Phys. **A672**, 387 (2000).
[17] T. Yamaya *et al.*, Phys. Rev. C **42**, 1935 (1990); Prog. Theor. Phys. Suppl. **132**, 73 (1998).
[18] F. Michel, F. Brau, G. Reidemeister, and S. Ohkubo, Phys. Rev. Lett. **85**, 1823 (2000); F. Michel, G. Reidemeister, and S. Ohkubo, Phys. Rev. C **63**, 034620 (2001).
[19] M.P. Nicoli, Ph.D. thesis, Strasbourg, 1998.
[20] J. Aguilar *et al.*, Commun. Math. Phys. **22**, 269 (1971); E. Balslev *et al.*, *ibid.* **22**, 280 (1971); B. Simon, *ibid.* **27**, 1 (1971).
[21] M.L. Halbert *et al.*, Phys. Lett. **51B**, 341 (1974).
[22] G. Gaul, W. Bickel, W. Lammer, and R. Santo, *Resonances in Heavy Ion Reactions*, Lecture Note in Physics Vol. 156 (Springer-Verlag, Berlin, 1982).
[23] M. Gai *et al.*, Phys. Rev. Lett. **47**, 1878 (1981).
[24] S. Ohkubo, Y. Hirabayashi, and T. Sakuda, Phys. Rev. C **57**, 2760 (1998); T. Sakuda and S. Ohkubo, Prog. Theor. Phys. Suppl. **132**, 103 (1998).
[25] N. Cindro, Ann. Phys. (Paris) **13**, 289 (1988).
[26] N. Curtis *et al.*, Phys. Rev. C **53**, 1804 (1996).
[27] K. Morita *et al.*, Phys. Rev. Lett. **55**, 185 (1985).
[28] R.B. Firestone *et al.*, *Table of Isotopes* (Wiley, New York, 1996).